ACS central science

http://pubs.acs.org/journal/acscii

Research Article

Mucins Inhibit Coronavirus Infection in a Glycan-Dependent Manner

Casia L. Wardzala, Amanda M. Wood, David M. Belnap, and Jessica R. Kramer*

Cite This: *ACS Cent. Sci.* 2022, 8, 351−360

Read Online

ACCESS | Metrics & More | Article Recommendations | Supporting Information

ABSTRACT: Mucins are a diverse and heterogeneous family of glycoproteins that comprise the bulk of mucus and the epithelial glycocalyx. Mucins are intimately involved in viral transmission. Mucin and virus laden particles can be expelled from the mouth and nose to later infect others. Viruses must also penetrate the mucus layer before cell entry and replication. The role of mucins and their molecular structure have not been well-characterized in coronavirus transmission studies. Laboratory studies predicting high rates of fomite transmission have not translated to real-world infections, and mucins may be one culprit. Here, we probed both surface and direct contact transmission scenarios for their dependence on mucins and their structure. We utilized disease-causing, bovine-derived, human coronavirus OC43. We found that bovine mucins could inhibit the infection of live cells in a concentration- and glycan-dependent manner. The effects were observed in both mock fomite and direct contact transmission experiments and were not dependent upon surface material or time-on-surface. However, the effects were abrogated by removal of the glycans or in a cross-species infection scenario where bovine mucin could not inhibit the infection of a murine coronavirus. Together, our data indicate that the mucin molecular structure plays a complex and important role in host defense.

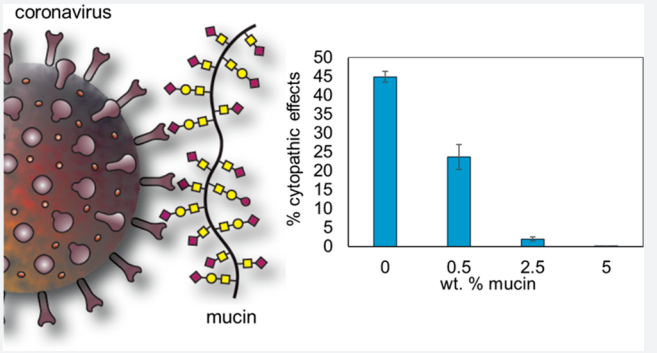

INTRODUCTION

Coronaviruses (CoVs) have emerged as a serious public health threat due to their ability to cause respiratory disease, including severe acute respiratory syndrome (SARS), gastroenteritis, neurological disease, and additional diseases in humans and other animals. SARS-CoV infected more than 8000 people between 2002 and 2003, and since 2012, the Middle East respiratory syndrome (MERS) virus has infected more than 1700 people.[1] Since January 2020, the devastating SARS-CoV-2 virus and its related disease COVID-19 has killed more than 4 million people worldwide.[2,3] During the course of these outbreaks, researchers have sought to understand routes and mechanisms of transmission. Respiratory viruses can spread through direct contact with bodily fluids or from an infected individual's cough, sneeze, or vocalization that expels airborne particles from their mucus membranes.[4−8] Airborne virus can land directly on the next host's mucus membranes or can be deposited onto a nearby surface creating a fomite object.[9] Virus can be transferred from the fomite to a new host's mucosal tissues, and the viral replication cycle ensues. Here, we present data regarding the role that mucus proteins play in CoV infection.

The fomite transmission scenario particularly piqued our interest due to conflicting reports on its importance throughout the COVID-19 pandemic and other disease outbreaks. Several epidemiological case studies indicated that common touch surfaces were a source of fomite transmission that led to outbreak infections of CoVs and other viruses.[10−15] Laboratory research had also indicated that CoVs can persist on surfaces for days[16−20] and even weeks[21−24] in both model and clinical settings. However, large-scale epidemiology studies[25−27] have now led public health experts to conclude that fomite transmission of CoVs, including SARS-CoV-2, is of relatively low risk.[9,28] Such discrepancies have frustrated public health messaging and resulted in misallocation of resources toward the excessive disinfection of surfaces,[29] which comes with its own potential respiratory dangers.[30,31]

Evaluating viral viability on surfaces in a model setting is advantageous since it is challenging to fully eliminate human behavior leading to direct contact or airborne transmission. However, confounding factors must be at play since the predictions of laboratory studies failed to actualize. The assay method is one factor since the simple detection of viral genetic material by polymerase chain reaction (PCR) cannot reveal if the virus is intact and viable.[32−35] Recent reviews summarize more enlightening studies indicating that fomite-sourced CoVs are viable and infectious to live human cells even after weeks

Received: November 7, 2021
Published: February 14, 2022

dry on surfaces.[21,36] It was noted that viral titers might be in excess of real-world scenarios, which could lead to disproportionately high survival.[27] However, we noted another important factor that could be at play. Coughs and sneezes expel virus encased in mucus or mucosalivary fluid, and viruses must pass through host mucus before entering cells to replicate. However, prior studies typically utilized buffers or growth media without accounting for mucus. We wondered if mucus could, at least partially, explain the discrepancy between real-world low fomite transmission and the reported persistent viability of CoVs on surfaces in laboratory settings.

Mucus is an aqueous solution of 5−10 wt % mucin glycoproteins with traces of salts, lipids, DNA, and other proteins.[37,38] Similarly, mucosalivary fluid contains 0.3−3 wt % mucin.[39,40] Mucins are a family of anionic high-molecular-weight secreted and cell-surface proteins characterized by remarkably dense regions of Pro and heavily glycosylated Thr and Ser (Figure 1).[41] The mucin peptide backbone provides

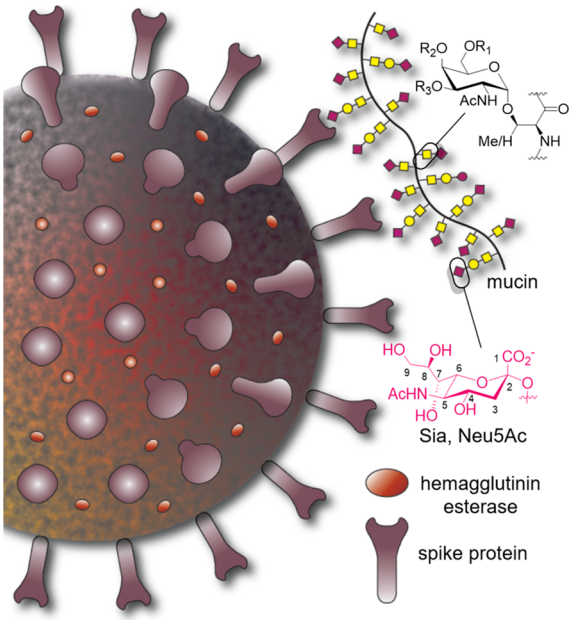

Figure 1. Coronavirus and mucin structure where viral spike proteins bind to mucin Sia glycans. Mucin glycosylation initiates at Ser/Thr with αGalNAc, and variable extended glycans often terminate in Sia, Neu5Ac, which can be further acetylated at positions 4, 7, 8, and 9. Some coronaviruses bind Sia via hemagglutinin esterase.

rigid structural support while the glycans bind copious water and bind to biological targets, including pathogens. We hypothesized that mucins could play a role in CoV fomite viability by affecting the local environment experienced by viruses in drying droplets or by binding them directly. The viability of influenza and polio in evaporating droplets was found to be dependent upon hydration, pH, and salt, which mucins will affect, and mucins have shown inhibitory effects against the cell entry of many viruses including influenza, polio, herpes, and human immunodeficiency viruses in culture models.[42−45]

Mucus has largely been viewed as a simple hydrating barrier material, including in its role in viral defense.[42,46] However, the engagement of mucin glycans has emerged as an important factor in host defense against broad classes of pathogens including viruses, bacteria, and fungi.[47,48] Mammalian mucin glycan patterns vary with species and tissue[49,50] and commonly terminate in sialic acid structures (Sias).[51−53] Sias are also termed neuraminic acids (Neus) due to their concurrent identification in saliva and in the brain. 50+ Sia forms have been identified with varied acetylation patterns or other structural variations (Figure 1).[54,55] Since mucins are the first point of contact when a virus is inhaled or inadvertently transferred to a mucus membrane, it is intuitive that CoVs have evolved the ability to bind to Sias as part of their replication strategy. In fact, Sias have been identified as binding targets of more than 9 disease-causing CoV strains.[55−61]

CoVs are enveloped RNA viruses that must deliver their nucleocapsid into the host cell to replicate.[62] Some CoVs use cell-surface mucin Sias to induce membrane fusion with host cells, while others bind for adhesion but enter via other surface proteins.[55,56,58,60,61,63] For example, SARS-CoV-2 and MERS-CoV bind Sias but use angiotensin converting enzyme 2 or dipeptidyl peptidase 4, respectively, for cellular entry. The Sia-binding strategy is not unique to CoVs, and their conserved receptor has an architecture similar to the influenza virus receptor that engages Sias to gain cell entry.[56,64] CoVs have two surface projections, spike and hemagglutinin-esterase (HE) proteins. The spike protein is usually responsible for Sia binding and host fusion, though in some cases binding occurs on HE (Figure 1).[65] Considering the potential physical and biochemical properties of mucin−virus interactions, we sought to probe the role of mucins in CoV infectivity.

RESULTS

CoV Selection and Infectivity Assay Design. To investigate the role of mucins in CoV transmission, we selected human CoV OC43 for the bulk of our studies. CoVs are divided into α, β, γ, and δ genera. OC43, like SARS-CoV, SARS-CoV-2, and MERS-CoV, is a β-CoV that binds Sia via its spike protein. OC43 is endemic in the human population, causing mild respiratory tract infections with the potential for severe complications or even fatalities in young children, the elderly, or immunocompromised individuals.[66,67] The virus originated relatively recently via zoonotic transmission from a bovine CoV.[68,69] Both OC43 and the related bovine CoV are reported to bind 5,9-*O*-acetyl-Sia (9AcOSia, Neu5,9Ac) and 5-*O*-acetyl-Sia (5AcOSia, Neu5Ac) via their spike proteins.[70−72] Based on this knowledge, we selected bovine submaxillary mucin for our studies since the commercially available material is known to contain Neu5Ac and Neu5,9Ac and originates from a tissue of native viral targeting.[73,74]

We sought to examine the effects of varied mucin concentration on OC43 infectivity. To generate the fomites, viral stocks were diluted in phosphate buffered saline (PBS), complete media, or solutions supplemented with mucin. We selected concentrations from 0.1 to 5 wt % mucin to represent the range naturally found in mucus and saliva. Droplets of 2 μL were placed on a surface and allowed to dry completely. After ca. 5 min, fomites were rehydrated with complete media and the solutions subjected to infectivity assays in Vero E6 cells. We quantified the protein concentration before and after recovering virus from plastic fomites both with and without mucin (Figure S15). We found that the rehydration and recovery of the CoV from the plastic surface was highly efficient in both cases and that adsorption and loss of the virus were not a factor in our results. For direct contact transmission, we simply added virus to cellular growth media supplemented with mucin.

https://doi.org/10.1021/acscentsci.1c01369
ACS Cent. Sci. 2022, 8, 351−360

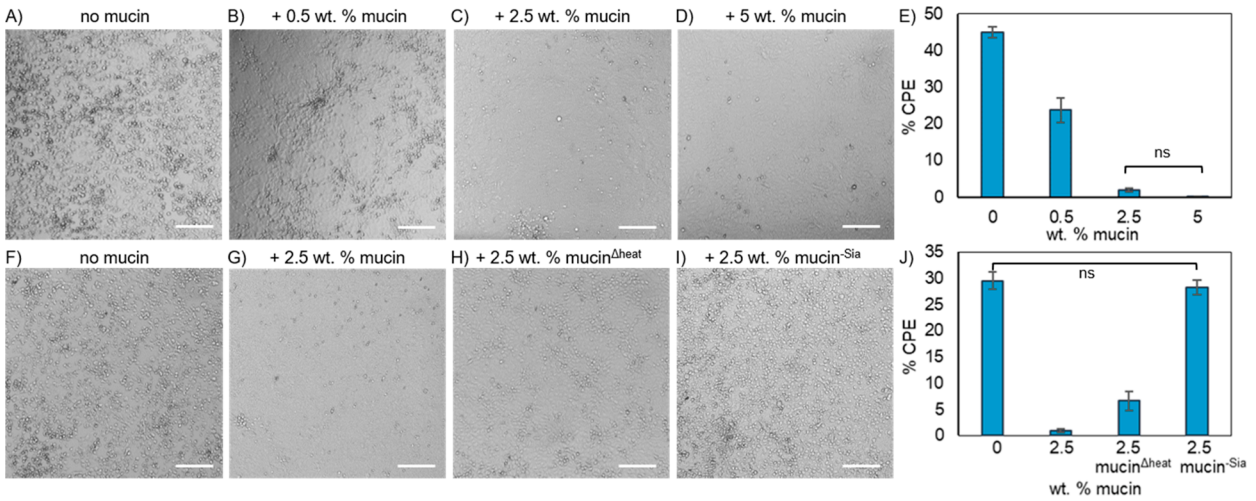

Figure 2. Mucins inhibit the infection of live cells by CoV OC43 in a concentration- and glycan-dependent manner. CPE is evidenced by morphological changes where infected cells rise above the healthy cell monolayer below. (A–D, F–I) 10× bright-field images of CPE in a $TCID_{50}$ assay in Vero E6 cells 5 days postinfection, 10^{-1} dilution. Mucin$^{\Delta heat}$ is heat-denatured mucin, and mucin^{-Sia} is sialidase-treated mucin. Scale bars are 200 μm. (E, J) Quantitated relative CPE due to OC43 infection in Vero E6 cells by image analysis software. All data are presented as mean values and their associated standard error calculated from an N of 4–6. Data were processed with ANOVA and Tukey tests. Panels E and J only show correlations that were nonsignificant. All other correlations were statistically different at $p > 0.05$ or less.

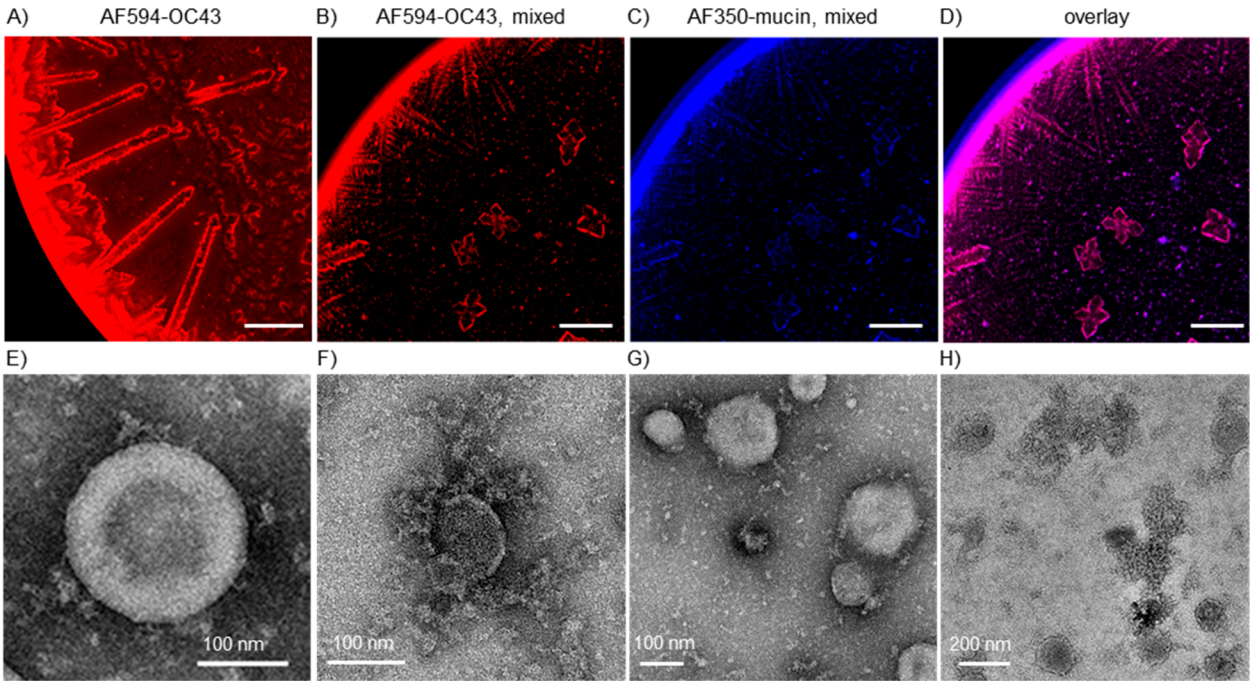

Figure 3. Mucins physically associate with CoV OC43. 10× fluorescent microscopy images of plastic fomites formed from 2 μL simulated sneeze droplets with viral stock at 10% v/v and 0.5 wt % mucin in media: (A) AF594-OC43 alone; (B) AF594-OC43 mixed solution; (C) AF350-mucin, mixed solution; and (D) overlaid images of panels B and C. Scale bars are 200 μm. (E–H) TEM images of mucin-coated OC43 viruses.

We conducted 50% tissue culture infectious dose per milliliter ($TCID_{50}$) and plaque assays. In both assays, a confluent monolayer of host cells is infected with serial dilutions of the virus. For the $TCID_{50}$ assay, morphological changes are observed upon infection or cell death, termed cytopathic effects (CPE). The dilution at which 50% of the cell samples show CPE is used to calculate the $TCID_{50}$ of the viral titer. We imaged the cells for CPE at 5 days postinfection using bright-field microscopy. To better quantify and compare $TCID_{50}$ results between assays, we used image analysis software to quantify the percent of cells displaying CPE. In a confluent monolayer of healthy cells, extrusion is part of the natural response to crowding, and not all cells extended above the monolayer are due to CPE.[75] Therefore, we corrected for this in our image analysis (Figure S1). For plaque assays, infected host cells are covered with an immobilizing overlay medium (agarose) to prevent infection from spreading through the liquid medium during propagation.[76] Zones of cell death, or plaques, will develop. After fixing and staining with crystal violet, plaques are counted, and viral titers are reported in terms of plaque forming units (PFUs) per milliliter. Data are presented as mean values and their associated standard error

https://doi.org/10.1021/acscentsci.1c01369
ACS Cent. Sci. 2022, 8, 351–360

calculated along with ANOVA and Tukey analyses (see the SI). Experiments were generally performed in triplicate and were reproducible over 3+ separate experiments.

Effect of Mucins on CoV Infectivity in Fomite Transmission on Plastic. Plastic-fomite-derived OC43 remained highly infectious after drying in media or PBS (Figure 2A; see Figure S2). However, OC43 fomites dried in media or PBS supplemented with mucin revealed a remarkable decrease in CPE that scaled with increasing wt % mucin (Figure 2B−E, Figures S3 and S4). An addition of just 0.5 wt % mucin reduced the CPE by 52% as compared to media alone. CPE was essentially eliminated by supplementation with 2.5 or 5 wt % mucin, which reduced CPE by 95.6% and 99.9%, respectively, over the standard 5 day assay window. We continued observation through 7 days postinfection, and very minimal CPE expansion could be seen in the 2.5 wt % sample but not in the 5 wt % sample (see Figure S4). Plaque assays in Vero E6 cells also revealed a stark contrast between infectivities of CoV fomites prepared with and without mucin (see Figure S18 for plaque assay data). Clearly, the presence of mucin in these simulated cough or sneeze droplets has a significant effect on the ability of the CoVs to later infect cells.

Mucins and CoV OC43 Physically Associate. We sought to probe the mechanism by which mucins exert their protective effects against OC43 infection from plastic fomites. To directly image fomite structures, we used *N*-hydroxysuccinimide chemistry to fluorescently label the mucins with AF350 and OC43 with AF594.[77] Next, AF350-mucin and AF594-OC43 were dissolved separately or in combination in PBS, and fomites on plastic were prepared. As shown in Figure 3, mucins did not associate with the salt crystals dispersed over the plastic surface when dried alone (Figure S17) or in combination with OC43 (Figure 3C). Rather, a majority of the mucins localize to the dry droplet edge in a sort of coffee-ring effect. However, OC43 localization differed when dried alone vs with mucin. OC43 dried in PBS rather uniformly coats the salt crystal surfaces (Figure 3A). When coevaporated with mucin, however, the majority of the AF594-OC43 colocalized with the mucin ring, with only a small fraction coating the crystalline salt surfaces (Figure 3B,D). These data suggest that OC43 preferentially interacts with the mucin.

To further probe the physical association of OC43 and bovine mucin, we directly imaged them using transmission electron microscopy (TEM). OC43 was first concentrated by ultracentrifugation through a sucrose cushion. OC43, 2.5 wt % mucin, or OC43 + 2.5 wt % mucin solutions were prepared in PBS. The solutions were placed on the TEM grid for approximately 1 min to allow particle deposition, and then, excess solution was removed. Deposited virus and mucin were coated with negative stain, dried, and then imaged. We observed spherical OC43 virus and globular mucin glycoprotein aggregates when imaged alone (see Figure S22). In the case of the mixed mucin and virus samples, we observed what appears to be mucins coating the surface of the OC43 viruses (Figure 3E−H). These data further indicate that mucins and CoV OC43 physically interact.

Infection Inhibition Is Dependent on Mucin Glycans. Mucins have both biophysical and biochemical properties in terms of their rodlike, hydrophilic structure and glycans that can bind directly to CoVs. Mucins also have hydrophobic domains that aid in the formation of mucus gel networks.[37,78] The hydrophobic viral envelope could associate with these domains in the mucin, resulting in the colocalization effect we observed. In contrast to our data in Figure 2, Marr and co-workers studied the effect of relative humidity on droplets loaded with fluorescently labeled bacteriophage Φ6, lipids, and mucin. They reported that the Φ6 virus, which is also enveloped, was not associated with mucin in dry droplets.[79] Since these bacteriophages are not known to bind to mucin glycans, we wondered if mucin Sias could be at least partially responsible for the differing effects we observed with our fomites.

To test the Sia hypothesis, we quantified the total Sia content of our bovine submaxillary mucin using a colorimetric quantitation kit (see the SI). We found a Sia content of 0.036 ± 0.02 nmol/μg. Next, we treated the mucin with a commercially available sialidase, which enzymatically cleaves Sia glycans. Reaction products were again analyzed with the quantitation kit, and complete Sia removal was confirmed. We refer to this sample as mucin^{-Sia}. Residual sialidase was deactivated by brief heat-treatment to prevent any activity with OC43 or Vero cells. We also subjected Sia-containing mucin to brief heat-treatment (mucin$^{\Delta heat}$) to determine if protein denaturation or disruption of hydrophobic-associated networks would affect the ability of the mucin to protect cells from viral infection.

Mucin$^{\Delta heat}$ and mucin^{-Sia} and were utilized in OC43 fomite preparation on plastic, along with no mucin and untreated mucin controls. The fomites were rehydrated and subjected to $TCID_{50}$ assays in Vero cells and CPE image analysis. As expected, strong CPE was observed in the fomites generated from media with no mucin, while the addition of 2.5 wt % mucin essentially eliminated the CPE (Figure 2F,G,J, CPE reduced by 97%). Heat-treating the mucins resulted in only a minor recovery of infectivity (Figure 2H,J, 78% reduction in CPE), indicating that mucin conformation and/or intermolecular associations play only a small role in their protective effects. However, the removal of Sia from the mucins resulted in a near-total loss of the protective effects and a full recovery of infectivity (Figure 2I,J, 4% reduction in CPE), as differences in the two were not statistically significant. From these data, we can infer that Sia residues play a key role in the protective effects of mucin against OC43 CoV infection. Prior work by Szczepanski and co-workers similarly found that a global removal of Sia from whole cells reduced CoV adhesion and that supplementing the growth media with free Sia does not.[71] We can likely attribute such findings to the mucins in solution and in the glycocalyx.

Glycan patterns could affect mucin biophysics since they alter rigidity, hydration, and surface charge,[51,80−83] and therefore, assigning all effects to Sia−CoV binding could be erroneous due to neglecting conformational effects. Therefore, we examined the secondary structure of the untreated mucin, mucin$^{\Delta heat}$, and mucin^{-Sia} by circular dichroism spectroscopy. We found that untreated mucin was 72% helical (see Figure S9). Mucin$^{\Delta heat}$ and mucin^{-Sia} also displayed a helical character, though it was reduced to 53% and 41%, respectively. Since the removal of Sia and heat-treatment does induce a minor loss of the helical structure, we cannot definitively rule out conformational effects. However, mucin^{-Sia} was subjected to the same heat-treatment as mucin$^{\Delta heat}$ (in order to deactivate remaining sialidase) and experiences a much more dramatic loss of protective effects. Therefore, we propose glycan−virus binding as the major factor.

https://doi.org/10.1021/acscentsci.1c01369
ACS Cent. Sci. 2022, 8, 351−360

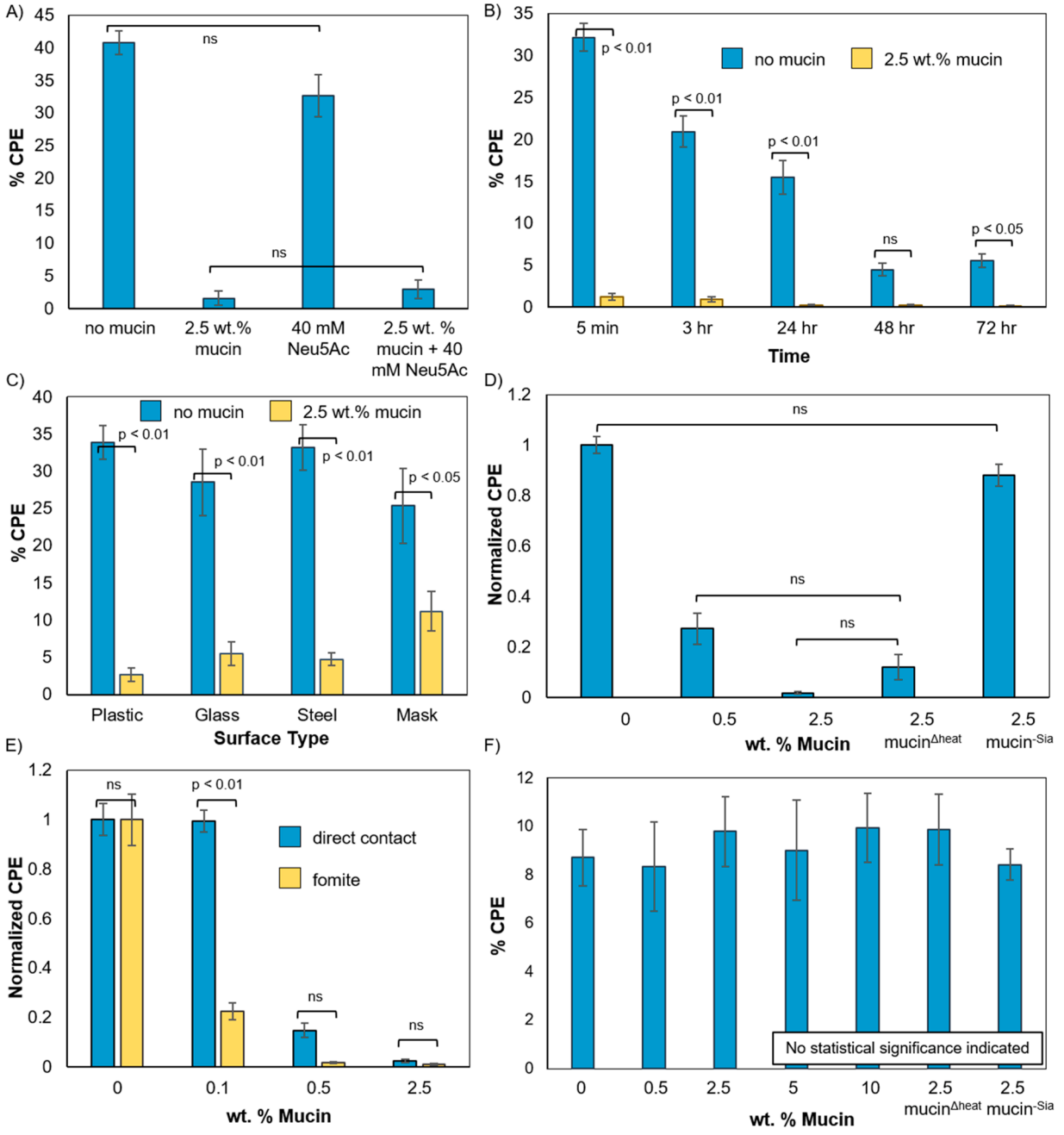

Figure 4. The inhibition of CoV fomite infection by mucins is independent of time and surface material but is dependent on attached Sias and on mucin−CoV species match. Mucins also inhibit infection in mock direct contact transmission. Quantitated relative CPE in $TCID_{50}$ assays in (A−E) Vero E6 cells infected with OC43 or (F) L2 mouse fibroblasts infected with MHV. Panels A−C and F are fomite transmission with simulated sneeze droplets, while panel D is direct contact transmission, and (E) is the comparison. Panels A, B, E, and F are data generated from plastic fomites, while panel C is data of fomites of common touch surfaces. In panel B, viral fomites were rehydrated at various time points. For panels D and E, CPE has been normalized to the no-mucin control. $Mucin^{\Delta heat}$ is heat-denatured while $mucin^{-Sia}$ is sialidase-treated. All data are presented as mean values and their associated standard error calculated from an N of 4−6. Data were processed with ANOVA and Tukey tests. One-way ANOVA of the data in panel F revealed no statistical significance. Panels A and D only show correlations that were nonsignificant. All other correlations were statistically different at $p > 0.05$ or less. Panels B, C, and E show correlations between no mucin and +2.5 wt % mucin and direct contact and fomite transmission, respectively.

To further probe the effects of Sia binding, we conducted infectivity experiments with mucin vs free small-molecule Sia (Neu5Ac) or in combination. We prepared plastic fomites using OC43 solutions in media, media + 2.5 wt % mucin, media + 40 mM Neu5Ac, or media + 2.5 wt % mucin and 40 mM Neu5Ac. Virus was rehydrated and subjected to $TCID_{50}$ assays in Vero E6 cells. Reproducibly, OC43 infectivity was high with no mucin and essentially eliminated with 2.5 wt % mucin (Figure 4A, Figure S10). Supplementation with 40 mM Neu5Ac only reduced infectivity by 20.1%, indicating that the multivalent display of the glycans from the mucin peptide backbone is essential for the inhibitory affects against infection. We did not observe any competition effect by combining 40 mM Neu5Ac with mucin, and the mucins still exerted their

https://doi.org/10.1021/acscentsci.1c01369
ACS Cent. Sci. 2022, 8, 351−360

protective effects. We could not examine the effects of Neu5,9Ac in this work since this Sia form is not currently commercially available in a pure form.

We further characterized the glycan-dependent interaction of mucin and OC43 in binding assays. We first examined three blocking agents on Nunc Maxisorp plates and selected bovine serum albumin (BSA) as having the lowest viral binding background (using AF594-OC43) as compared to milk and serum. We also coated plates with varied concentrations of AF350-mucin in order to determine the saturation concentration, which was 20 μg/mL mucin (see Figure S16). The following experiments were conducted using plates coated with 20 μg/mL mucin, mucin$^{\Delta heat}$, or mucin^{-Sia} and blocked with BSA. We utilized plates with no mucin, blocked with BSA treated with the same ELISA conditions as a control, and subtracted this background from all other results. Plates were incubated with varied concentrations of OC43 at 34 °C for 1 h. We employed an enzyme-linked immunoassay (ELISA) with a murine antibody (Ab) against OC43 and an antimouse Ab-horseradish peroxidase (HRP) conjugate for detection. As expected, we found high relative levels of mucin−OC43 binding for intact mucin that scaled with increasing virus concentration (Figure 5). Removal of the Sia groups essentially

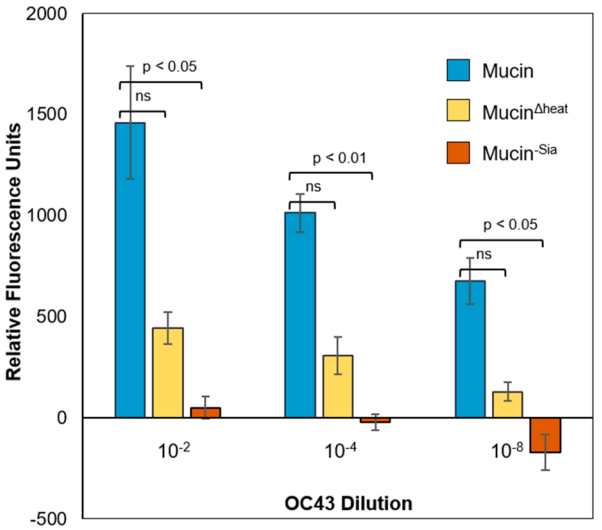

Figure 5. ELISA data for glycan-dependent mucin−CoV binding. Varied concentrations of CoV OC43 were incubated with surface-bound mucin, mucin$^{\Delta heat}$, mucin^{-Sia}, or no-mucin control (BSA only). Binding was detected by treatment with a murine anti-OC43 Ab followed by an antimouse-HRP Ab conjugate. Fluorescence is reported relative to the no-mucin control. All data are presented as mean values and their associated standard error calculated from an *N* of 4−6. Data were processed with ANOVA and Tukey tests. Graph shows correlations between mucin and mucin$^{\Delta heat}$ /mucin^{-Sia}.

eliminated viral binding. This correlates nicely with our infectivity assay results indicating that the inhibition phenomenon is indeed due to Sia−CoV binding. Also paralleling our infection assay data, heat denaturation of the mucin reduced, but did not eliminate, binding. Considering the reduction in binding due to heat-treatment, we speculate that conformational aspects of Sia presentation are important for mucin−CoV binding. We could directly visualize mucin−virus binding using AF594-OC43 (see Figure S17). These data indicate that AF594 labeling of the virus does not disrupt binding and that the morphology and localization of dry mucin−virus on plastic fomites as presented in Figure 2 are likely relevant to real-world structures.

Effect of Mucin on CoV Infectivity in Direct Contact Transmission. During our initial studies on plastic fomites, we noticed an interesting phenomenon with serial dilutions of rehydrated OC43 for plaque and $TCID_{50}$ assays. In these assays, infection rates typically go down as the viral titer is reduced by dilution. However, in the cases of mucin supplementation, we noticed that infectivity was lower in the most concentrated stock, increased in the next dilution, and then decreased serially with dilution thereafter. We surmised this was due to the presence of mucins in solution carried forward from the fomite preparation. Solution mucin concentration would be high in the first stock but then become diluted with the serial stocks. To confirm this hypothesis, we conducted the same plastic fomite experiment with cell media supplemented with constant wt % mucin. Indeed, viral infectivity in the $TCID_{50}$ assay scaled as expected where infectivity decreased with the serial dilutions (see Figure S12).

Considering the interesting flux in infectivity that appeared to be due to the action of fomite-sourced mucins in solution, we hypothesized that mucins would also affect infectivity in a mock direct contact transmission experiment. Therefore, we next addressed if the drying and concentrating step is essential for inhibition of CoV infection by mucins, or if they are also protective in direct contact transmission scenarios. For these experiments, we conducted $TCID_{50}$ assays and CPE image analysis in Vero E6 cells at various viral dilutions and with media supplemented with 0.5 or 2.5 wt % mucin, or with 2.5 wt % mucin$^{\Delta heat}$ or mucin^{-Sia}. In these cases, the virus had never been dried, and cultured cells were treated with aliquots of mucin and CoV to mimic contact transmission at the mucosal membrane. As shown in Figure 4D, mucins are also highly protective in direct contact scenarios. Note that Figure 4D shows only correlations that were nonsignificant. We also observed the same glycan-dependent phenomena where heat-denatured mucins were still highly protective, but mucins that had been sialidase-treated did not inhibit infection. We compared the protective effects of mucin in the fomite vs direct contact experiments by normalizing the CPE of the no-mucin controls (Figure 4E). We noted that, at 0.1 and 0.5 wt % mucin, considering standard error alone, infection prevention was stronger in fomites than in direct contact but the difference for the 0.5 wt % experiment was not statistically significant by the Tukey test. With 2.5 wt % mucin, infection was essentially nullified in both cases. We speculate that in drying droplets the localized concentration of mucin will become very high, improving binding between mucin and virus.

Effect of Mucin on CoV Infectivity in Fomite Transmission over Time and on Various Surface Materials. Considering the strongly protective effects of bovine mucin against cellular infection by CoV OC43 from plastic fomites, we wondered if the same effects would be observed on other common touch surface materials and how long the effects would last. We first investigated whether time remaining dried on a surface plays a role in viral infectivity with or without mucins. We prepared plastic fomites as previously described for OC43 with both the media control and media + 2.5 wt % mucin. Viruses were rehydrated at 5 min or 3, 24, 48, or 72 h and the solutions subjected to $TCID_{50}$ assays and CPE image analysis in Vero E6 cells. As shown in Figure 4B, OC43

https://doi.org/10.1021/acscentsci.1c01369
ACS Cent. Sci. 2022, 8, 351−360

dried without mucin declines in infectivity by 82% over 3 days but does remain infectious. However, for the simulated sneeze droplets with mucin, we observed very little CPE from the 5 min dry sample (96% reduction from 5 min with no mucin) which declined to essentially nil by 24 h (99% reduction from 5 min with no mucin; Figure 4B, see Figure S20). This indicates that the detrimental effects of the mucin on viral viability are not affected by the time on the surface.

Next, we sought to ascertain if the protective effects of mucin against OC43 infection were isolated to plastic fomites, or if they would extend to other common touch surfaces. We selected steel, glass, and surgical masks for comparison to plastic. Fomites were again prepared using OC43 viral stocks diluted in media or media + 0.5 or 2.5 wt % mucin. Surface-adhered viruses were rehydrated and subjected to both $TCID_{50}$ with image analysis and plaque assays in Vero cells. For all surfaces tested, we observed strong CPE and high PFU counts in cells infected with virus dried without mucin (Figure 4C, plaque assay data are in Figure S18). By contrast, strong reductions in CPE were observed for virus dried with 2.5 wt % mucin regardless of the hard surface material. On plastic, CPE was reduced by 92%; on glass, by 81%; and on steel, by 86% as compared to the no-mucin control. Little to no reduction in CPE was observed with 0.5 wt % mucin.

In agreement with other studies, the porous surface of the surgical mask had slightly less infectious virus overall as compared to plastic, glass, and steel in both the plaque and $TCID_{50}$ assays (Figure 4C, Figures S18 and S19).[16−23] On this material, the protective effects of mucin were tempered, and only a 56% reduction in CPE was observed. We presume that this is due to rapid dissolution of the aqueous virus solution across the high surface area of the mask fibers. This would prevent the mucin and virus from concentrating together as effectively as on a hard surface where they can form the ring structure shown in Figure 3. This could result in the reduction of protective effects. Interestingly, a study on the survival of influenza on paper currency indicated that infectivity was higher with mucus than without[84] which researchers presumed was due to preventing desiccation of the virus.[85] We did not observe such an effect here.

Cross-Species Mucin−Virus Pair Does Not Offer Infection Protection. We hypothesized that Neu5Ac- and Neu5,9Ac-spike protein binding is responsible for the bulk of the protective effects of bovine mucin against OC43 infection. The loss of these effects and return of infectivity with an application of sialidase-treated mucin support this hypothesis. However, sialidase removes all forms of Sia, and therefore, we cannot definitively confirm that the effects are due to Neu5Ac and Neu5,9Ac. To probe this theory from another angle, we investigated a murine β-CoV, mouse hepatitis virus (MHV). MHV is reported as selective for Neu4,5Ac, which bovine mucin has not been characterized to display, and MHV was specifically reported to not bind to bovine mucin.[86,87] Additionally, unlike OC43, MHV binds Sia via its HE protein rather than spike and enters cells via a non-Sia target protein (carcinoembryonic antigen-related cell adhesion molecule 1).[65] We prepared plastic fomites with either the media control or media + 0.5, 2.5, or 5.0 wt % mucin as previously described. We also included an even higher concentration of 10.0 wt % mucin, and we prepared samples with +2.5 wt % $mucin^{-Sia}$ or $mucin^{\Delta heat}$. MHV was rehydrated, and the solutions were subjected to $TCID_{50}$ assays with image analysis in murine fibroblast L2 cells. As shown in Figure 4F and Figure S21, the addition of any mucin form or in any concentration had no effect on MHV infectivity, even at the highest 10 wt % concentration. These data further support the hypothesis that the protective effects of bovine mucin against OC43 are related to Sia-specific spike binding.

CONCLUSION AND PERSPECTIVES

Mucins are at the forefront of epithelial defense. The classical view of their mechanism of action is as a simple, hydrating barrier both in mucus and at the cell surface within the glycocalyx. However, in recent years, it has become apparent that both mucin biophysics and biochemistry are dependent upon small changes in their structures and glycoforms.[46] Mucin glycan patterns are unique to each species and tissue and dynamically respond to genetic, environmental, and metabolic cues.[49,50] We have now shown that mucins play a role in defense against CoV infection in a manner dependent upon their Sia glycans.

OC43 is a disease-causing human CoV that is structurally related to the bovine CoV from which it originated. We found that bovine mucins could inhibit OC43 infection but could not inhibit infection by a mouse CoV, MHV. We speculate that this is due to CoV binding of the species-specific Sia variants found on the bovine mucin, but further work is required to assign causality. Glycan characterization is a challenging field in its own right, requiring specialized equipment and training. Enzymatic removal of the Sia residues from the bovine mucins eliminated their protective effects against OC43, but heat denaturation did not. We also noted that free Sia in solution offered little infection protection, indicating that the glycans must be attached to the mucin peptide backbone for these effects. This aligns with data indicating that free Neu5,9Ac can bind to OC43 but does not induce fusogenic conformational changes.[56] Our own binding assays indicate that OC43 binds directly to mucins in a glycan-dependent manner, and that a disturbance of protein structure and glycan presentation and orientation may disrupt binding.

We focused mainly on fomite transmission scenarios due to real-world epidemiology data indicating low transmission by this route conflicting with lab data reporting remarkably prolonged CoV viability on surfaces. We suspect that mucins, which had been largely ignored in laboratory models, are a culprit in the discrepancy. We found that mucins are protective against fomite transmission from many common touch surface materials and that the effect does not diminish over time. Mucins also inhibited infection in a mock direct contact transmission experiment where the virus had never been dried. In this case, cells were bathed in mucin solution to mimic the mucosal tissue surface.

We suspect that these inhibitory effects are not unique to OC43 since SARS-CoV, SARS-CoV-2, and MERS are all reported to bind Sias.[58,88,89] Cell entry of SARS-CoV-2 has been shown to be mediated by cell-surface Sias, and the spike protein can bind several human Sias.[90,91] Interestingly, human Sia levels and forms can vary with diet[92] and with respiratory-relevant diseases such as cystic fibrosis[93] and lung cancer.[94] CoV−Sia binding could potentially contribute to the vulnerability of certain populations to infection or influence superspreading phenomena.[95] Collectively, these data indicate that we are just scratching the surface of the complex biochemical actions of the fascinating glycoprotein mucins that broadly defend against infection.

https://doi.org/10.1021/acscentsci.1c01369
ACS Cent. Sci. 2022, 8, 351−360

■ ASSOCIATED CONTENT

Supporting Information

. The Supporting Information is available free of charge at https://pubs.acs.org/doi/10.1021/acscentsci.1c01369.

Detailed experimental procedures and additional supporting data including representative microscopy images of CPE in $TCID_{50}$ assays and CPE analysis data, plaque assay data, circular dichroism spectroscopy data, TEM images, binding assay data, and statistical analyses (PDF)

■ AUTHOR INFORMATION

Corresponding Author

Jessica R. Kramer − *Department of Biomedical Engineering, University of Utah, Salt Lake City, Utah 84112, United States;* orcid.org/0000-0002-4268-0126; Email: jessica.kramer@utah.edu

Authors

Casia L. Wardzala − *Department of Biomedical Engineering, University of Utah, Salt Lake City, Utah 84112, United States*

Amanda M. Wood − *Department of Biomedical Engineering, University of Utah, Salt Lake City, Utah 84112, United States*

David M. Belnap − *Department of Biochemistry and School of Biological Sciences, University of Utah, Salt Lake City, Utah 84112, United States*

Complete contact information is available at: https://pubs.acs.org/10.1021/acscentsci.1c01369

Author Contributions

Project conception: J.R.K. and C.L.W. Experimental design: all authors. Data collection: C.L.W., A.M.W., and D.M.B. Supervision: J.R.K. Editing/review: all authors.

Notes

The authors declare no competing financial interest.

■ ACKNOWLEDGMENTS

We thank Dr. Stephen Goldstein for helpful discussions regarding viral protocols. We thank the lab of Prof. Nels Elde for the gift of OC43 and MHV and the lab of Prof. Michael Yu for the use of their circular dichroism spectrometer. C.L.W. was supported by a National Science Foundation Graduate Research Fellowship. This work was supported by National Science Foundation RAPID DMR-2026965 (J.R.K.).

■ REFERENCES

(1) Li, F. Structure, Function, and Evolution of Coronavirus Spike Proteins. *Annu. Rev. Virol.* **2016**, *3* (1), 237−261.

(2) Hui, D. S.; I Azhar, E.; Madani, T. A.; Ntoumi, F.; Kock, R.; Dar, O.; Ippolito, G.; Mchugh, T. D.; Memish, Z. A.; Drosten, C.; et al. The Continuing 2019-NCoV Epidemic Threat of Novel Coronaviruses to Global Health — The Latest 2019 Novel Coronavirus Outbreak in Wuhan, China. *Int. J. Infect. Dis.* **2020**, *91*, 264−266.

(3) WHO media. *WHO Health Emergency Dashboard WHO (COVID-19) Homepage*. https://covid19.who.int/ (accessed Jan. 27, 2022).

(4) Kutter, J. S.; Spronken, M. I.; Fraaij, P. L.; Fouchier, R. A.; Herfst, S. Transmission Routes of Respiratory Viruses among Humans. *Curr. Opin. Virol.* **2018**, *28*, 142−151.

(5) Stadnytskyi, V.; Bax, C. E.; Bax, A.; Anfinrud, P. The Airborne Lifetime of Small Speech Droplets and Their Potential Importance in SARS-CoV-2 Transmission. *Proc. Natl. Acad. Sci. U. S. A.* **2020**, *117* (22), 11875−11877.

(6) Bazant, M. Z.; Bush, J. W. M. A Guideline to Limit Indoor Airborne Transmission of COVID-19. *Proc. Natl. Acad. Sci. U. S. A.* **2021**, *118* (17), No. e2018995.

(7) Echternach, M.; Gantner, S.; Peters, G.; Westphalen, C.; Benthaus, T.; Jakubaß, B.; Kuranova, L.; Döllinger, M.; Kniesburges, S. Impulse Dispersion of Aerosols during Singing and Speaking: A Potential COVID-19 Transmission Pathway. *Am. J. Respir. Crit. Care Med.* **2020**, *202* (11), 1584−1587.

(8) Wang, C. C.; Prather, K. A.; Sznitman, J.; Jimenez, J. L.; Lakdawala, S. S.; Tufekci, Z.; Marr, L. C. Airborne Transmission of Respiratory Viruses. *Science 80* **2021**, *373*, No. eabd9149.

(9) Meyerowitz, E. A.; Richterman, A.; Gandhi, R. T.; Sax, P. E. Transmission of SARS-CoV-2: A Review of Viral, Host, and Environmental Factors. *Ann. Intern. Med.* **2021**, *174*, 69.

(10) Gwaltney, J. M.; Hendley, J. O. Transmission of Experimental Rhinovirus Infection by Contaminated Surfaces. *Am. J. Epidemiol.* **1982**, *116* (5), 828−33.

(11) Brlek, A.; Vidovič, S.; Vuzem, S.; Turk, K.; Simonović, Z. Possible Indirect Transmission of COVID-19 at a Squash Court, Slovenia, March 2020: Case Report. *Epidemiol. Infect.* **2020**, *148*, No. e120.

(12) Abbas, M.; Robalo Nunes, T.; Martischang, R.; Zingg, W.; Iten, A.; Pittet, D.; Harbarth, S. Nosocomial Transmission and Outbreaks of Coronavirus Disease 2019: The Need to Protect Both Patients and Healthcare Workers. *Antimicrob. Resist. Infect. Control* **2021**, *10* (1), 7.

(13) Xie, C.; Zhao, H.; Li, K.; Zhang, Z.; Lu, X.; Peng, H.; Wang, D.; Chen, J.; Zhang, X.; Wu, D.; et al. The Evidence of Indirect Transmission of SARS-CoV-2 Reported in Guangzhou, China. *BMC Public Health* **2020**, *20* (1), 1202.

(14) Liu, J.; Huang, J.; Xiang, D. Large SARS-CoV-2 Outbreak Caused by Asymptomatic Traveler, China. *Emerg. Infect. Dis.* **2020**, *26* (9), 2260−2263.

(15) Lessells, R.; Moosa, Y.; De Oliveira, T. *Report into a nosocomial outbreak of coronavirus disease 2019 (COVID-19) at Netcare St. Augustine's Hospital*. https://www.krisp.org.za/news.php?id=421(pdf) (accessed Jan. 27, 2022).

(16) Duan, S. M.; Zhao, X. S.; Wen, R. F.; Huang, J. J.; Pi, G. H.; Zhang, S. X.; Han, J.; Bi, S. L.; Ruan, L.; Dong, X. P. Stability of SARS Coronavirus in Human Specimens and Environment and Its Sensitivity to Heating and UV Irradiation. *Biomed. Environ. Sci.* **2003**, *16* (3), 246−255.

(17) Rabenau, H. F.; Cinatl, J.; Morgenstern, B.; Bauer, G.; Preiser, W.; Doerr, H. W. Stability and Inactivation of SARS Coronavirus. *Med. Microbiol. Immunol.* **2005**, *194*, 1−6.

(18) van Doremalen, N.; Bushmaker, T.; Morris, D. H.; Holbrook, M. G.; Gamble, A.; Williamson, B. N.; Tamin, A.; Harcourt, J. L.; Thornburg, N. J.; Gerber, S. I.; et al. Aerosol and Surface Stability of SARS-CoV-2 as Compared with SARS-CoV-1. *N. Engl. J. Med.* **2020**, *382* (16), 1564−1567.

(19) Warnes, S. L.; Little, Z. R.; Keevil, C. W. Human Coronavirus 229E Remains Infectious on Common Touch Surface Materials. *MBio* **2015**, *6* (6), e01697−e01715.

(20) Kratzel, A.; Steiner, S.; Todt, D.; V'kovski, P.; Brueggemann, Y.; Steinmann, J.; Steinmann, E.; Thiel, V.; Pfaender, S. Temperature-Dependent Surface Stability of SARS-CoV-2. *J. Infect.* **2020**, *81* (3), 452−482.

(21) Ren, S. Y.; Wang, W. B.; Hao, Y. G.; Zhang, H. R.; Wang, Z. C.; Chen, Y. L.; Gao, R. D. Stability and Infectivity of Coronaviruses in Inanimate Environments. *World J. Clin. Cases* **2020**, *8* (8), 1391−1399.

(22) Riddell, S.; Goldie, S.; Hill, A.; Eagles, D.; Drew, T. W. The Effect of Temperature on Persistence of SARS-CoV-2 on Common Surfaces. *Virol. J.* **2020**, *17*, 145.

(23) Liu, Y.; Li, T.; Deng, Y.; Liu, S.; Zhang, D.; Li, H.; Wang, X.; Jia, L.; Han, J.; Bei, Z.; et al. Stability of SARS-CoV-2 on Environmental Surfaces and in Human Excreta. *J. Hosp. Infect.* **2021**, *107*, 105−107.

(24) Kampf, G.; Todt, D.; Pfaender, S.; Steinmann, E. Persistence of Coronaviruses on Inanimate Surfaces and Its Inactivation with Biocidal Agents. *J. Hosp. Infect.* **2020**, *104* (3), 246−251.
(25) Mondelli, M. U.; Colaneri, M.; Seminari, E. M.; Baldanti, F.; Bruno, R. Low Risk of SARS-CoV-2 Transmission by Fomites in Real-Life Conditions. *Lancet Infect. Dis.* **2021**, *21* (5), No. e112.
(26) Horoho, S.; Musik, S.; Bryant, D.; Brooks, W.; Porter, I. M. Questioning COVID-19 Surface Stability and Fomite Spreading in Three Aeromedical Cases: A Case Series. *Mil. Med.* **2021**, *186* (7−8), e832−e835.
(27) Goldman, E. Exaggerated Risk of Transmission of COVID-19 by Fomites. *Lancet Infect. Dis.* **2020**, *20* (8), 892−893.
(28) Center for Disease Control and Prevention; National Center for Immunization and Respiratory Diseases (NCIRD); Division of Viral Diseases. *Science Brief: SARS-CoV-2 and Surface (Fomite) Transmission for Indoor Community Environments*. https://www.cdc.gov/coronavirus/2019-ncov/more/science-and-research/surface-transmission.html (accessed Aug. 15, 2021).
(29) Lewis, D. COVID-19 Rarely Spreads through Surfaces. So Why Are We Still Deep Cleaning? *Nature* **2021**, *590*, 26−28.
(30) Zock, J. P.; Plana, E.; Jarvis, D.; Antó, J. M.; Kromhout, H.; Kennedy, S. M.; Künzli, N.; Villani, S.; Olivieri, M.; Torén, K.; et al. The Use of Household Cleaning Sprays and Adult Asthma: An International Longitudinal Study. *Am. J. Respir. Crit. Care Med.* **2007**, *176* (8), 735−41.
(31) Zock, J. P.; Plana, E.; Antó, J. M.; Benke, G.; Blanc, P. D.; Carosso, A.; Dahlman-Höglund, A.; Heinrich, J.; Jarvis, D.; Kromhout, H.; et al. Domestic Use of Hypochlorite Bleach, Atopic Sensitization, and Respiratory Symptoms in Adults. *J. Allergy Clin. Immunol.* **2009**, *124* (4), 731−738.
(32) Chia, P. Y.; Coleman, K. K.; Tan, Y. K.; Ong, S. W. X.; Gum, M.; Lau, S. K.; Lim, X. F.; Lim, A. S.; Sutjipto, S.; Lee, P. H.; et al. Detection of Air and Surface Contamination by SARS-CoV-2 in Hospital Rooms of Infected Patients. *Nat. Commun.* **2020**, *11* (1), 2800.
(33) Wei, L.; Huang, W.; Lu, X.; Wang, Y.; Cheng, L.; Deng, R.; Long, H.; Zong, Z. Contamination of SARS-CoV-2 in Patient Surroundings and on Personal Protective Equipment in a Non-ICU Isolation Ward for COVID-19 Patients with Prolonged PCR Positive Status. *Antimicrob. Resist. Infect. Control* **2020**, *9* (1), 167.
(34) Chan, V. W. M.; So, S. Y. C.; Chen, J. H. K.; Yip, C. C. Y.; Chan, K. H.; Chu, H.; Chung, T. W. H.; Sridhar, S.; To, K. K. W.; Chan, J. F. W.; et al. Air and Environmental Sampling for SARS-CoV-2 around Hospitalized Patients with Coronavirus Disease 2019 (COVID-19). *Infect. Control Hosp. Epidemiol.* **2020**, *41* (11), 1258−1265.
(35) Colaneri, M.; Seminari, E.; Novati, S.; Asperges, E.; Biscarini, S.; Piralla, A.; Percivalle, E.; Cassaniti, I.; Baldanti, F.; Bruno, R.; et al. Severe Acute Respiratory Syndrome Coronavirus 2 RNA Contamination of Inanimate Surfaces and Virus Viability in a Health Care Emergency Unit. *Clin. Microbiol. Infect.* **2020**, *26* (8), 1094.e1−1094.e5.
(36) Aydogdu, M. O.; Altun, E.; Chung, E.; Ren, G.; Homer-Vanniasinkam, S.; Chen, B.; Edirisinghe, M. Surface Interactions and Viability of Coronaviruses: Surface Interactions and Viability of Coronaviruses. *J. R. Soc. Interface* **2021**, *18* (174), 20200798.
(37) Bansil, R.; Turner, B. S. Mucin Structure, Aggregation, Physiological Functions and Biomedical Applications. *Curr. Opin. Colloid Interface Sci.* **2006**, *11* (2−3), 164−170.
(38) Creeth, J. M. Constituents of Mucus and Their Separation. *Br. Med. Bull.* **1978**, *34* (1), 17−24.
(39) Acquier, A. B.; Pita, A. K. D. C.; Busch, L.; Sánchez, G. A. Comparison of Salivary Levels of Mucin and Amylase and Their Relation with Clinical Parameters Obtained from Patients with Aggressive and Chronic Periodontal Disease. *J. Appl. Oral Sci.* **2015**, *23* (3), 288−294.
(40) Schipper, R. G.; Silletti, E.; Vingerhoeds, M. H. Saliva as Research Material: Biochemical, Physicochemical and Practical Aspects. *Arch. Oral. Biol.* **2007**, *52*, 1114−1135.
(41) UniProt Consortium, T. UniProt: The Universal Protein Knowledgebase. *Nucleic Acids Res.* **2018**, *46* (5), 2699.
(42) Lieleg, O.; Lieleg, C.; Bloom, J.; Buck, C. B.; Ribbeck, K. Mucin Biopolymers as Broad-Spectrum Antiviral Agents. *Biomacromolecules* **2012**, *13*, 1724−1732.
(43) Schaffer, F. L.; Soergel, M. E.; Straube, D. C. Survival of Airborne Influenza Virus: Effects of Propagating Host, Relative Humidity, and Composition of Spray Fluids. *Arch. Virol.* **1976**, *51* (4), 263−273.
(44) Benbough, J. E. Some Factors Affecting the Survival of Airborne Viruses. *J. Gen. Virol.* **1971**, *10* (3), 209−220.
(45) Yang, W.; Elankumaran, S.; Marr, L. C. Relationship between Humidity and Influenza A Viability in Droplets and Implications for Influenza's Seasonality. *PLoS One* **2012**, *7* (10), No. e46789.
(46) Linden, S. K.; Sutton, P.; Karlsson, N. G.; Korolik, V.; McGuckin, M. A. Mucins in the Mucosal Barrier to Infection. *Mucosal Immunol* **2008**, *1* (3), 183−197.
(47) Werlang, C. A.; Chen, W. G.; Aoki, K.; Wheeler, K. M.; Tymm, C.; Mileti, C. J.; Burgos, A. C.; Kim, K.; Tiemeyer, M.; Ribbeck, K. Mucin O-Glycans Suppress Quorum-Sensing Pathways and Genetic Transformation in Streptococcus Mutans. *Nat. Microbiol.* **2021**, *6*, 574−583.
(48) Wheeler, K. M.; Cárcamo-Oyarce, G.; Turner, B. S.; Dellos-Nolan, S.; Co, J. Y.; Lehoux, S.; Cummings, R. D.; Wozniak, D. J.; Ribbeck, K. Mucin Glycans Attenuate the Virulence of Pseudomonas Aeruginosa in Infection. *Nat. Microbiol.* **2019**, *4*, 2146−2154.
(49) Hattrup, C. L.; Gendler, S. J. Structure and Function of the Cell Surface (Tethered) Mucins. *Annu. Rev. Physiol.* **2008**, *70*, 431−457.
(50) Guzman-Aranguez, A.; Woodward, A. M.; Pintor, J.; Argüeso, P. Targeted Disruption of Core 1 B1,3-Galactosyltransferase (C1galt1) Induces Apical Endocytic Trafficking in Human Corneal Keratinocytes. *PLoS One* **2012**, *7* (5), No. e36628.
(51) Henrissat, B.; Surolia, A.; Stanley, P. A Genomic View of Glycobiology. In *Essentials of Glycobiology*; Cold Spring Harbor Laboratory Press, 2009.
(52) Gendler, S. J. MUC1, The Renaissance Molecule. *J. Mammary Gland Biol. Neoplasia* **2001**, *6* (3), 339−353.
(53) Arike, L.; Hansson, G. C. The Densely O-Glycosylated MUC2Mucin Protects the Intestine and Provides Food for the Commensal Bacteria. *J. Mol. Biol.* **2016**, *428*, 3221−3229.
(54) Varki, A.; Schnaar, R. L.; Schauer, R. Sialic Acids and Other Nonulosonic Acids. In *Essentials of Glycobiology*; Cold Spring Harbor Laboratory Press: Cold Spring Harbor, NY, 2015; pp 2015−2017.
(55) Park, S. S. Post-Glycosylation Modification of Sialic Acid and Its Role in Virus Pathogenesis. *Vaccines* **2019**, *7* (4), 171.
(56) Tortorici, M. A.; Walls, A. C.; Lang, Y.; Wang, C.; Li, Z.; Koerhuis, D.; Boons, G.-J.; Bosch, B.-J.; Rey, F. A.; de Groot, R. J.; et al. Structural Basis for Human Coronavirus Attachment to Sialic Acid Receptors. *Nat. Struct. Mol. Biol.* **2019**, *26* (6), 481−489.
(57) Schwegmann-Weßels, C.; Bauer, S.; Winter, C.; Enjuanes, L.; Laude, H.; Herrler, G. The Sialic Acid Binding Activity of the S Protein Facilitates Infection by Porcine Transmissible Gastroenteritis Coronavirus. *Virol. J.* **2011**, *8*, 1−7.
(58) Li, W.; Hulswit, R. J. G.; Widjaja, I.; Raj, V. S.; McBride, R.; Peng, W.; Widagdo, W.; Tortorici, M. A.; Van Dieren, B.; Lang, Y.; et al. Identification of Sialic Acid-Binding Function for the Middle East Respiratory Syndrome Coronavirus Spike Glycoprotein. *Proc. Natl. Acad. Sci. U. S. A.* **2017**, *114* (40), E8508−E8517.
(59) Huang, X.; Dong, W.; Milewska, A.; Golda, A.; Qi, Y.; Zhu, Q. K.; Marasco, W. A.; Baric, R. S.; Sims, A. C.; Pyrc, K.; et al. Human Coronavirus HKU1 Spike Protein Uses O -Acetylated Sialic Acid as an Attachment Receptor Determinant and Employs Hemagglutinin-Esterase Protein as a Receptor-Destroying Enzyme. *J. Virol.* **2015**, *89* (14), 7202−7213.
(60) Shahwan, K.; Hesse, M.; Mork, A. K.; Herrler, G.; Winter, C. Sialic Acid Binding Properties of Soluble Coronavirus Spike (S1) Proteins: Differences between Infectious Bronchitis Virus and Transmissible Gastroenteritis Virus. *Viruses* **2013**, *5* (8), 1924−1933.

(61) Wasik, B. R.; Barnard, K. N.; Parrish, C. R. Effects of Sialic Acid Modifications on Virus Binding and Infection. *Trends Microbiol* **2016**, *24* (12), 991−1001.
(62) Belouzard, S.; Millet, J. K.; Licitra, B. N.; Whittaker, G. R. Mechanisms of Coronavirus Cell Entry Mediated by the Viral Spike Protein. *Viruses* **2012**, *4* (6), 1011−1033.
(63) Krempl, C.; Ballesteros, M. L.; Zimmer, G.; Enjuanes, L.; Klenk, H. D.; Herrler, G. Characterization of the Sialic Acid Binding Activity of Transmissible Gastroenteritis Coronavirus by Analysis of Haemagglutination-Deficient Mutants. *J. Gen. Virol.* **2000**, *81*, 489−496.
(64) Barnard, K. N.; Wasik, B. R.; Laclair, J. R.; Buchholz, D. W.; Weichert, W. S.; Alford-Lawrence, B. K.; Aguilar, H. C.; Parrish, C. R. Expression of 9-o-and 7,9-o-Acetyl Modified Sialic Acid in Cells and Their Effects on Influenza Viruses. *MBio* **2019**, *10* (6), 1−17.
(65) Langereis, M. A.; van Vliet, A. L. W.; Boot, W.; de Groot, R. J. Attachment of Mouse Hepatitis Virus to O-Acetylated Sialic Acid Is Mediated by Hemagglutinin-Esterase and Not by the Spike Protein. *J. Virol.* **2010**, *84* (17), 8970−8974.
(66) Isaacs, D.; Flowers, D.; Clarke, J. R.; Valman, H. B.; MacNaughton, M. R. Epidemiology of Coronavirus Respiratory Infections. *Arch. Dis. Child.* **1983**, *58* (7), 500−503.
(67) Su, S.; Wong, G.; Shi, W.; Liu, J.; Lai, A. C. K.; Zhou, J.; Liu, W.; Bi, Y.; Gao, G. F. Epidemiology, Genetic Recombination, and Pathogenesis of Coronaviruses. *Trends Microbiol* **2016**, *24* (6), 490−502.
(68) Vijgen, L.; Keyaerts, E.; Moës, E.; Thoelen, I.; Wollants, E.; Lemey, P.; Vandamme, A.-M.; Van Ranst, M. Complete Genomic Sequence of Human Coronavirus OC43: Molecular Clock Analysis Suggests a Relatively Recent Zoonotic Coronavirus Transmission Event. *J. Virol.* **2005**, *79* (3), 1595−1604.
(69) Lau, S. K. P.; Lee, P.; Tsang, A. K. L.; Yip, C. C. Y.; Tse, H.; Lee, R. A.; So, L.-Y.; Lau, Y.-L.; Chan, K.-H.; Woo, P. C. Y.; et al. Molecular Epidemiology of Human Coronavirus OC43 Reveals Evolution of Different Genotypes over Time and Recent Emergence of a Novel Genotype Due to Natural Recombination. *J. Virol.* **2011**, *85* (21), 11325−11337.
(70) Vlasak, R.; Luytjes, W.; Spaan, W.; Palese, P. Human and Bovine Coronaviruses Recognize Sialic Acid-Containing Receptors Similar to Those of Influenza C Viruses. *Proc. Natl. Acad. Sci. U. S. A.* **1988**, *85* (12), 4526−4529.
(71) Szczepanski, A.; Owczarek, K.; Bzowska, M.; Gula, K.; Drebot, I.; Ochman, M.; Maksym, B.; Rajfur, Z.; Mitchell, J. A.; Pyrc, K. Canine Respiratory Coronavirus, Bovine Coronavirus, and Human Coronavirus OC43: Receptors and Attachment Factors. *Viruses* **2019**, *11* (4), 328.
(72) Feuerbaum, S.; Saile, N.; Pohlentz, G.; Müthing, J.; Schmidt, H. De-O-Acetylation of Mucin-Derived Sialic Acids by Recombinant NanS-p Esterases of Escherichia Coli O157:H7 Strain EDL933. *Int. J. Med. Microbiol.* **2018**, *308* (8), 1113−1120.
(73) Schauer, R.; Srinivasan, G. V.; Wipfler, D.; Kniep, B.; Schwartz-Albiez, R. O-Acetylated Sialic Acids and Their Role in Immune Defense. In *Advances in Experimental Medicine and Biology*; Wu, A. M., Ed.; Springer Science+Business Media, LLC, 2011; Vol. *705*, pp 525−548.
(74) Wasik, B. R.; Barnard, K. N.; Ossiboff, R. J.; Khedri, Z.; Feng, K. H.; Yu, H.; Chen, X.; Perez, D. R.; Varki, A.; Parrish, C. R. Distribution of O-Acetylated Sialic Acids among Target Host Tissues for Influenza Virus. *mSphere* **2017**, *2* (5), e00379.
(75) Gudipaty, S. A.; Rosenblatt, J. Epithelial Cell Extrusion: Pathways and Pathologies. *Semin. Cell Dev. Biol.* **2017**, *67*, 132−140.
(76) Baer, A.; Kehn-Hall, K. Viral Concentration Determination through Plaque Assays: Using Traditional and Novel Overlay Systems. *J. Vis. Exp.* **2014**, *93*, 52065.
(77) Zhang, S. L. X.; Tan, H. C.; Hanson, B. J.; Ooi, E. E. A Simple Method for Alexa Fluor Dye Labelling of Dengue Virus. *J. Virol. Methods* **2010**, *167*, 172−177.
(78) Cone, R. A. Barrier Properties of Mucus. *Adv. Drug Delivery Rev.* **2009**, *61* (2), 75−85.
(79) Vejerano, E. P.; Marr, L. C. Physico-Chemical Characteristics of Evaporating Respiratory Fluid Droplets. *J. R. Soc. Interface* **2018**, *15* (139), 20170939.
(80) Majima, Y.; Harada, T.; Shimizu, T.; Takeuchi, K.; Sakakura, Y.; Yasuoka, S.; Yoshinaga, S. Effect of Biochemical Components on Rheologic Properties of Nasal Mucus in Chronic Sinusitis. *Am. J. Respir. Crit. Care Med.* **1999**, *160* (2), 421−426.
(81) Puchelle, E.; Zahm, J. M.; Havez, R. Biochemical and Rheological Data in Sputum. 3. Relationship between the Biochemical Constituents and the Rheological Properties of Sputum. *Bull. Physio-Pathol. Respir.* **1973**, *9* (2), 237−257.
(82) Chace, K. V.; Leahy, D. S.; Martin, R.; Carubelli, R.; Flux, M.; Sachdev, G. P. Respiratory Mucous Secretions in Patients with Cystic Fibrosis: Relationship between Levels of Highly Sulfated Mucin Component and Severity of the Disease. *Clin. Chim. Acta* **1983**, *132* (2), 143−155.
(83) Shogren, R.; Gerken, T. A.; Jentoft, N. Role of Glycosylation on the Conformation and Chain Dimensions of O-Linked Glycoproteins: Light-Scattering Studies of Ovine Submaxillary Mucin. *Biochemistry* **1989**, *28* (13), 5525−5536.
(84) Thomas, Y.; Vogel, G.; Wunderli, W.; Suter, P.; Witschi, M.; Koch, D.; Tapparel, C.; Kaiser, L. Survival of Influenza Virus on Banknotes. *Appl. Environ. Microbiol.* **2008**, *74* (10), 3002−3007.
(85) Parker, E. R.; Dunham, W. B.; Mac Neal, W. J. Resistance of the Melbourne Strain of Influenza Virus to Desiccation. *J. Lab. Clin. Med.* **1944**, *29* (1), 37−42.
(86) Li, Z.; Lang, Y.; Liu, L.; Bunyatov, M. I.; Sarmiento, A. I.; de Groot, R. J.; Boons, G. J. Synthetic O-Acetylated Sialosides Facilitate Functional Receptor Identification for Human Respiratory Viruses. *Nat. Chem.* **2021**, *13*, 496−503.
(87) Langereis, M. A.; Zeng, Q.; Heesters, B.; Huizinga, E. G.; de Groot, R. J. The Murine Coronavirus Hemagglutinin-Esterase Receptor-Binding Site: A Major Shift in Ligand Specificity through Modest Changes in Architecture. *PLoS Pathog* **2012**, *8* (1), No. e1002492.
(88) Sun, X.-L. The Role of Cell Surface Sialic Acids for SARS-CoV-2 Infection. *Glycobiology* **2021**, *31*, 1245−1253.
(89) Bò, L.; Miotto, M.; Di Rienzo, L.; Milanetti, E.; Ruocco, G. Exploring the Association Between Sialic Acid and SARS-CoV-2 Spike Protein Through a Molecular Dynamics-Based Approach. *Front. Med. Technol.* **2021**, *2*, 614652.
(90) Nguyen, L.; McCord, K. A.; Bui, D. T.; Bouwman, K. M.; Kitova, E. N.; Elaish, M.; Kumawat, D.; Daskhan, G. C.; Tomris, I.; Han, L.; et al. Sialic Acid-Containing Glycolipids Mediate Binding and Viral Entry of SARS-CoV-2. *Nat. Chem. Biol.* **2022**, *18*, 81−90.
(91) Dhar, C.; Sasmal, A.; Diaz, S.; Verhagen, A.; Yu, H.; Li, W.; Chen, X.; Varki, A. Are Sialic Acids Involved in COVID-19 Pathogenesis? *Glycobiology* **2021**, *31* (9), 1068−1071.
(92) Samraj, A. N.; Pearce, O. M. T.; Läubli, H.; Crittenden, A. N.; Bergfeld, A. K.; Band, K.; Gregg, C. J.; Bingman, A. E.; Secrest, P.; Diaz, S. L.; et al. A Red Meat-Derived Glycan Promotes Inflammation and Cancer Progression. *Proc. Natl. Acad. Sci. U. S. A.* **2015**, *112* (2), 542−547.
(93) Davril, M.; Degroote, S.; Humbert, P.; Galabert, C.; Dumur, V.; Lafitte, J. J.; Lamblin, G.; Roussel, P. The Sialylation of Bronchial Mucins Secreted by Patients Suffering from Cystic Fibrosis or from Chronic Bronchitis Is Related to the Severity of Airway Infection. *Glycobiology* **1999**, *9* (3), 311−321.
(94) Pearce, O. M. T.; Läubli, H. Sialic Acids in Cancer Biology and Immunity. *Glycobiology* **2016**, *26* (2), 111−128.
(95) Stein, R. A. Super-Spreaders in Infectious Diseases. *Int. J. Infect. Dis.* **2011**, *15* (8), 510−513.

https://doi.org/10.1021/acscentsci.1c01369
ACS Cent. Sci. 2022, 8, 351−360